

Instability of a thin viscous film flowing under an inclined substrate: the emergence and stability of rivulets - CORRIGENDUM

P.G. Ledda, G. Lerisson, G. Balestra and F. Gallaire

(Received xx; revised xx; accepted xx)

Recent developments revealed an error in Lerisson *et al.* (2020), which propagates into Ledda *et al.* (2020). The mistake, reconducted from Lerisson *et al.* (2020), stems from the fact that the normalization of the curvature involves two independent length scales, which we erroneously assumed to be identical in the rest of this series of papers. The presence of the parameter $\frac{h_N}{l_c} \sqrt{\sin \theta} = \frac{h_N}{\tilde{\ell}_c^*} = 1/\tilde{\ell}_c^*$, with $l_c = \sqrt{\frac{\gamma}{\rho g}}$, was overlooked and assumed to be $\tilde{\ell}_c^* = 1$. The correct expression of the full curvature reads:

$$\kappa = \frac{\frac{\partial^2 h}{\partial x^2} \left(1 + \left(\frac{h_N}{\tilde{\ell}_c^*} \frac{\partial h}{\partial y} \right)^2 \right) + \frac{\partial^2 h}{\partial y^2} \left(1 + \left(\frac{h_N}{\tilde{\ell}_c^*} \frac{\partial h}{\partial x} \right)^2 \right) - 2 \left(\frac{h_N}{\tilde{\ell}_c^*} \right)^2 \frac{\partial h}{\partial x} \frac{\partial h}{\partial y} \frac{\partial^2 h}{\partial x \partial y}}{\left(1 + \left(\frac{h_N}{\tilde{\ell}_c^*} \frac{\partial h}{\partial x} \right)^2 + \left(\frac{h_N}{\tilde{\ell}_c^*} \frac{\partial h}{\partial y} \right)^2 \right)^{3/2}}.$$

Since the incorrect expression was employed in Ledda *et al.* (2020) (equations (3.3) and (A1)), some clarifications should be made about the validity of the results.

The numerical simulations of Section 3.2 (and in particular Figure 3) are valid only for the case $\tilde{\ell}_c^* = 1$. However, the discussion about the effect of the linear advection velocity $u = \cot \theta \tilde{\ell}_c^*$ remains valid.

In Section 4, the performed linear stability analyses are valid again only for the case $\tilde{\ell}_c^* = 1$ (Figures 4, 5, 6, 7). For each value of $\tilde{\ell}_c^*$, a different rivulet profile is identified (see corrigendum of Lerisson *et al.* (2020)), and thus the statement about the uniqueness of the rivulet in Section 4.1 needs to be rectified. We complete the analysis by reporting in Figure 1 of this corrigendum the results of the linear temporal and spatial stability analyses for different values of $\tilde{\ell}_c^*$. We recall that the perturbation with respect to the rivulet profile is assumed of the form $\eta = \hat{\eta}(y) \exp[i(k_x x - \omega t)]$. The temporal stability analysis (i.e. $k_x \in \mathbb{R}$ is fixed and one looks for $\omega \in \mathbb{C}$) shows a reduction of the temporal growth rate $\text{Im}(\omega)$ as $\tilde{\ell}_c^*$ increases. This reduction yields to the complete quenching of the secondary instability for sufficiently large u and $\tilde{\ell}_c^*$ (Figure 1). Similarly, the spatial stability analysis (i.e. $\omega \in \mathbb{R}$ is fixed and one looks for $k_x \in \mathbb{C}$) shows an analogous reduction of the spatial growth rate $-\text{Im}(k_x)$ with $\tilde{\ell}_c^*$. In contrast, $\text{Re}(\omega)$ in the temporal approach and $\text{Re}(k_x)$ in the spatial one do not vary significantly with increasing $\tilde{\ell}_c^*$.

An increase of $\tilde{\ell}_c^*$ leads to a decrease of the film thickness and thus of the hydrostatic pressure gradients due to the gravity component normal to the substrate. As a consequence, the growth rates are reduced and the flow is thus stabilized. However, the quantities $\text{Re}(\omega)$ and $\text{Re}(k_x)$ are directly related to the advection of perturbations, which is dominated by u .

The results of Section 5 are updated with the corrected theoretical amplifications. Following the procedure outlined in the paper, the theoretical amplification follows the same trend as the experimental one, without the need to fit the initial amplitude at $x = 0$, that is now simply assumed to be the saturation value of the optical sensor, varying

slightly from one set of experiments to the other (see Figure 2 of this corrigendum). However, we have now included errorbars in Figure 2 of this corrigendum (replacing Figure 9 of the original paper), which reflect the relative tolerance in the measurement of Δ and h_N/ℓ_c of 15%. This relates to the experimental error due to the undersampling in the identification of the position of the maximum thickness of the rivulet, since the resolution in the spanwise location was ≈ 1 mm, while the rivulet thickness varies from $h = 1.5$ to $h = 1.7$ in a region of ≈ 1.5 mm extension. Besides, the relation (5.1)b of the original manuscript is now an approximation, since $1.65 < \max(h) < 1.71$ as $\tilde{\ell}_c^*$ varies, which gives a supplementary uncertainty of $\approx 4\%$ on $\max(h)$ and therefore on h_N .

Despite the assumptions reported in the paper and these uncertainties, the trends are very similar and thus the correlation between theoretical and experimental amplification is confirmed. We have also updated Figure 10 (Figure 3 of this corrigendum) to include the marginal stability threshold below which perturbations are damped. The experimental values of Δ and h_N/ℓ_c are mean values in the 15% uncertainty region mentioned earlier. A good agreement is observed between the theoretical onset of the instability and the growth of lenses on the rivulets. Note that the correlation between experiments and theory and the trends are more convincing in this corrected version than in the original manuscript. The main result of this corrigendum is the existence of a theoretical threshold below which rivulets are stable, in complement to the previous conclusions.

The results of Section 6 remain valid since in the linear and weakly non-linear models the curvature is linearized. While this does not modify the discussion, it should be specified in Figure 13 that the fully-non linear simulation was performed with $\tilde{\ell}_c^* = 1$.

Declaration of interests

The authors report no conflict of interest.

REFERENCES

- LEDDA, P. G., LERISSON, G., BALESTRA, G. & GALLAIRE, F. 2020 Instability of a thin viscous film flowing under an inclined substrate: the emergence and stability of rivulets. *Journal of Fluid Mechanics* **904**, A23.
- LERISSON, G., LEDDA, P. G., BALESTRA, G. & GALLAIRE, F. 2020 Instability of a thin viscous film flowing under an inclined substrate: steady patterns. *Journal of Fluid Mechanics* **898**, A6.

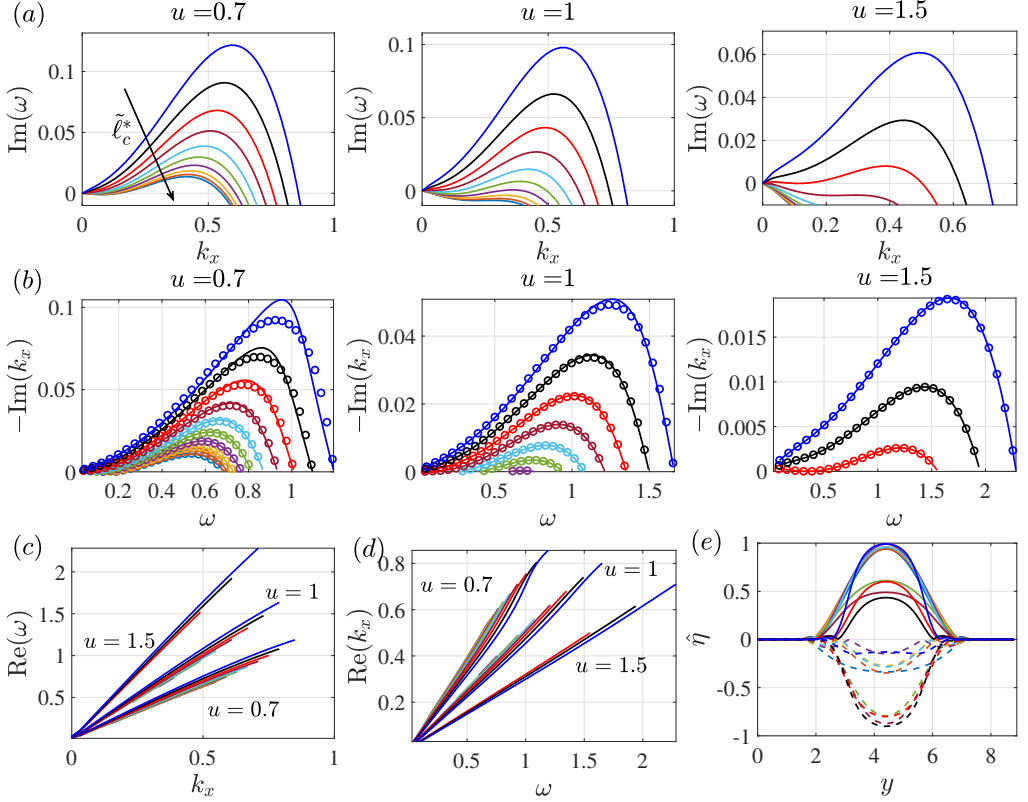


FIGURE 1. Results of the linear stability analysis for varying $\tilde{\ell}_c^*$. (a) Temporal stability analysis: temporal growth rate as a function of k_x . (b): Spatial growth rate from the spatial stability analysis (lines) and from the Gaster transformation (circles) as a function of ω . (c) Real part of the complex frequency from the temporal approach as a function of k_x . (d) Variation of $\text{Re}(k_x)$ with ω , for the spatial approach. (e) Most unstable mode for $u = 0.7$ and varying $\tilde{\ell}_c^*$, real (solid lines) and imaginary (dashed lines) parts, for the temporal approach. The different colours correspond to $\tilde{\ell}_c^* = 1$ (blue), $\tilde{\ell}_c^* = 1.1$ (black), $\tilde{\ell}_c^* = 1.25$ (red), $\tilde{\ell}_c^* = 1.43$ (maroon), $\tilde{\ell}_c^* = 1.67$ (cyan), $\tilde{\ell}_c^* = 2$ (green), $\tilde{\ell}_c^* = 2.5$ (purple), $\tilde{\ell}_c^* = 3.33$ (yellow), $\tilde{\ell}_c^* = 5$ (orange), $\tilde{\ell}_c^* = 10$ (light blue).

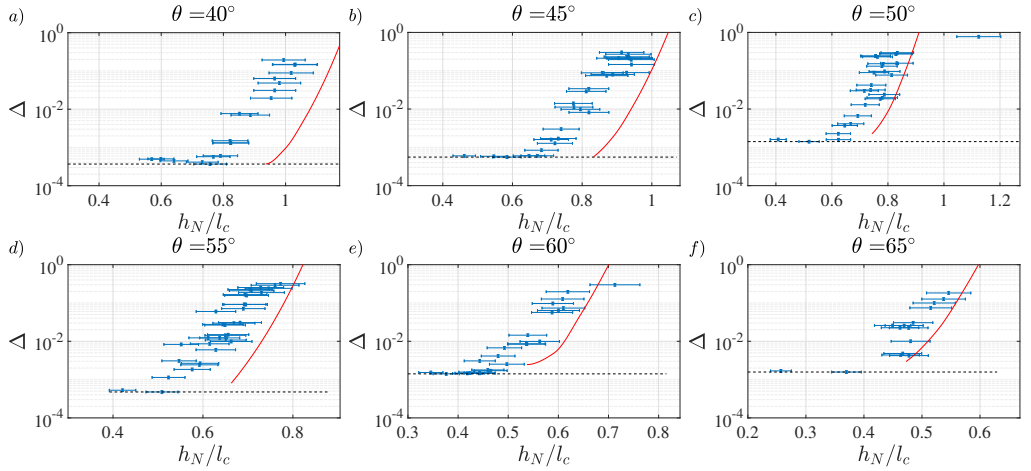


FIGURE 2. Values of Δ (blue dots) as a function of h_N/l_c , for different values of θ . The black horizontal line denotes the plateau value due to the resolution of the optical sensor. The red lines denote the amplification estimated using the spatial stability analysis of §4.4 and the size of the plate, i.e. $\Delta = \Delta_0 \exp(-\text{Im}(k_x)L)$, with initial amplitude the saturation value of the optical sensor.

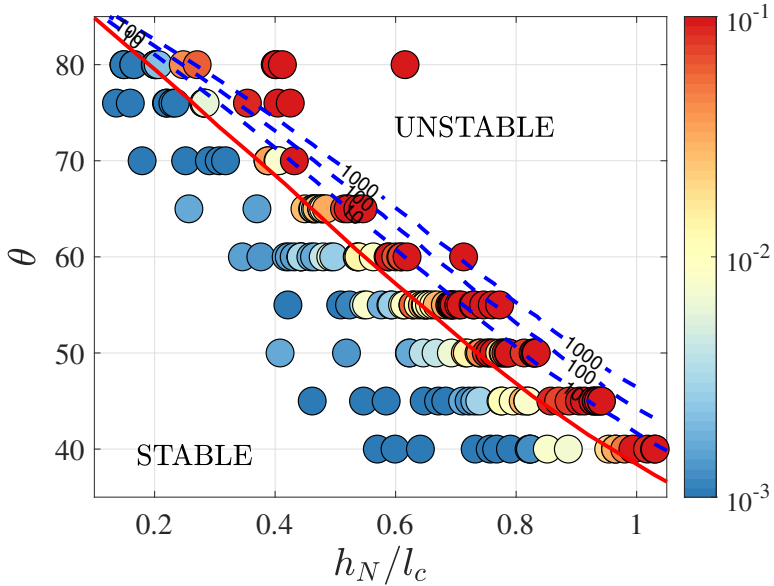


FIGURE 3. Results of the analysis in the $(\theta, h_N/l_c)$ plane: experimental measurements of Δ (coloured dots) and inlet disturbance amplification $\Delta/\Delta_0 = \exp(-\text{Im}(k_x)L)$ evaluated by the spatial stability analysis of Section 4.4 (blue iso-contours). The red solid line denotes the iso-contour $\text{Im}(\omega) = 0$, which identifies the marginal stability threshold.